Inorganic Chemistry

Article

pubs.acs.org/IC

Pincer-Ligated Nickel Hydridoborate Complexes: the Dormant Species in Catalytic Reduction of Carbon Dioxide with Boranes

Sumit Chakraborty, Jie Zhang, Yogi J. Patel, Jeanette A. Krause, and Hairong Guan*

Department of Chemistry, University of Cincinnati, P.O. Box 210172, Cincinnati, Ohio 45221-0172, United States

Supporting Information

ABSTRACT: Nickel pincer complexes of the type [2,6-$(R_2PO)_2C_6H_3$]NiH (R = ^{t}Bu, **1a**; R = ^{i}Pr, **1b**; R = ^{c}Pe, **1c**) react with BH_3·THF to produce borohydride complexes [2,6-$(R_2PO)_2C_6H_3$]Ni(η^2-BH_4) (**2a−c**), as confirmed by NMR and IR spectroscopy, X-ray crystallography, and elemental analysis. The reactions are irreversible at room temperature but reversible at 60 °C. Compound **1a** exchanges its hydrogen on the nickel with the borane hydrogen of 9-BBN or HBcat, but does not form any observable adduct. The less bulky hydride complexes **1b** and **1c**, however, yield nickel dihydridoborate complexes reversibly at room temperature when mixed with 9-BBN and HBcat. The dihydridoborate ligand in these complexes adopts an η^2-coordination mode, as suggested by IR spectroscopy and X-ray crystallography. Under the catalytic influence of **1a−c**, reduction of CO_2 leads to the methoxide level when 9-BBN or HBcat is employed as the reducing agent. The best catalyst, **1a**, involves bulky substituents on the phosphorus donor atoms. Catalytic reactions involving **1b** and **1c** are less efficient because of the formation of dihydridoborate complexes as the dormant species as well as partial decomposition of the catalysts by the boranes.

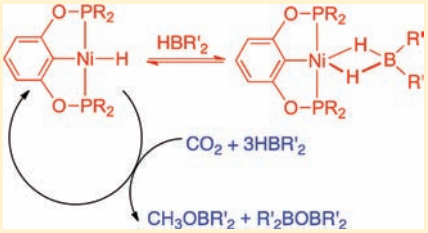

INTRODUCTION

We have recently reported an efficient nickel system for the catalytic reduction of CO_2 to the methoxide level under mild conditions using catecholborane (HBcat) as the reducing agent (eq 1).[1]

$$CO_2\ (1\ atm) + 3\ HBcat \xrightarrow[C_6D_6,\ RT]{cat.\ [Ni]H} catBOCH_3 + catBOBcat \quad (1)$$

[Ni]H =

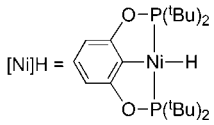

On the basis of NMR studies and density functional theory (DFT) calculations,[2] we have proposed a mechanism composed of three cycles (Scheme 1), of which each cycle decreases the formal oxidation state of carbon by 2 followed by the consumption of 1 equiv of HBcat to regenerate the active nickel hydride species. The computed free-energy profile of the entire process initially suggested to us that the reaction of [Ni]H with HCOOBcat (the first step of Cycle II) would cross the highest kinetic barrier.[2] We had therefore anticipated that replacing the bulky ^{t}Bu groups in the nickel pincer complex with smaller alkyl groups such as ^{i}Pr and ^{c}Pe (^{c}Pe = cyclopentyl) would accelerate the turnover-limiting step, leading to more efficient catalysis. Experimental results have shown that, on the contrary, analogous nickel complexes with a more accessible hydride moiety are, in fact, inferior catalysts.[3] This discrepancy may be reconciled by invoking an off-the-catalytic-loop adduct generated from the nickel hydride and HBcat (highlighted in red in Scheme 1). If this is the case, the structure of this adduct, the extent to which it forms, and the rate at which it releases the nickel hydride back to the catalytic cycles are all important in better understanding the catalytic system.

The literature has suggested many possible scenarios for the reaction of a transition metal hydride complex with a borane. If the metal center possesses a vacant coordination site, activation of the borane B−H bond leads to the formation of a σ-borane complex (structure **A** in Figure 1),[4,5] or a boryl dihydride complex (structure **B**, *endo* or *exo* isomer) as the oxidative addition product.[6] Abstraction of H^- by a Lewis acidic boron center gives rise to a metal complex bearing either a bidentate (structure **C**)[7] or a monodentate hydridoborate ligand (structure **D**).[8] Evolution of H_2 with concomitant formation of a metal-boryl species (structure **E**) is another possibility.[9] For the reactions involving HBcat, degradation of the borane by metal hydrides to $[B(cat)_2]^-$ has been previously observed.[10]

Prior to our work, there have been two reports pertaining to the reaction of a pincer-ligated nickel hydride complex and a borane, although the motivations for these studies are quite different from ours. To demonstrate that a Ni−BR'_2 moiety is capable of transferring boron to organic molecules, the Mindiola group has synthesized a PNP-pincer nickel boryl complex from the corresponding nickel hydride and HBcat (eq 2).[9b]

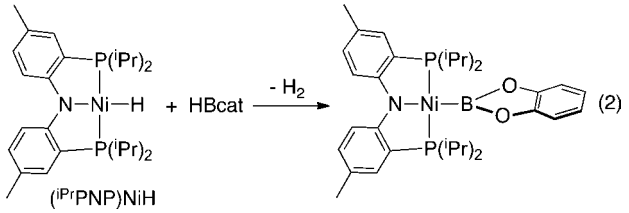

Received: March 20, 2012
Published: May 16, 2012

   dx.doi.org/10.1021/ic300587b | *Inorg. Chem.* 2013, 52, 37−47

Scheme 1. Proposed Mechanism for Nickel-Catalyzed Reduction of CO_2 with HBcat

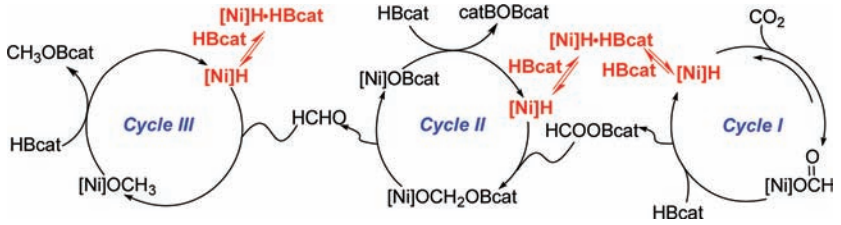

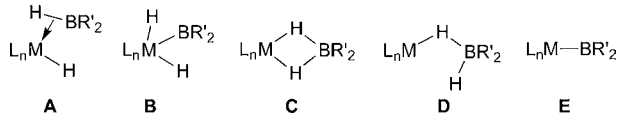

Figure 1. Possible products from the reaction of a transition metal hydride complex with a borane.

In a study of hydride affinity of BH_3 toward metal hydrides, Peruzzini and co-workers have recently investigated the interaction between a PCP-pincer nickel hydride and BH_3·THF, which yields a nickel borohydride complex as suggested by the NMR spectroscopy (eq 3).[8]

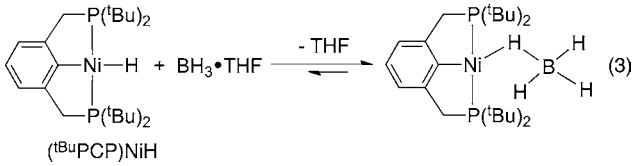

On the basis of DFT analyses, they have proposed a ground-state η^1-BH_4 structure, along with the η^2-BH_4 structure being the transition state that is responsible for the exchange between the bridging and terminal hydrogens. However, isolation of this nickel borohydride complex in the solid-state form has not been accomplished, mainly because of facile dissociation of BH_3 at temperatures that are convenient for workup.

In this paper, we will show unique reactivity of our POCOP-pincer nickel hydride complexes toward different boranes including BH_3·THF, 9-BBN, and HBcat (eq 4).

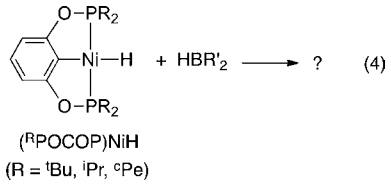

By varying the alkyl substituents on the phosphorus donor atoms of the pincer ligand, we will address how the size of the substituents impacts the reactivity of the nickel hydride complexes, as well as its relation with the efficiency of the nickel hydrides in catalyzing the reduction of CO_2 with boranes.

RESULTS AND DISCUSSION

Reactions of Nickel Hydride Complexes with BH_3·THF.

One obvious question is, how different could the reactivity toward boranes be for the POCOP-pincer complexes? The ν(CO) stretching frequencies of (^{tBu}POCOP)Ir(CO)[11] [1949 cm^{-1}] and (^{tBu}PCP)Ir(CO)[12] [1928 cm^{-1}] seem to support the notion that the POCOP-pincer ligand makes the metal center more electron deficient.[13] However, as suggested by Goldman and Krogh-Jespersen, the difference in ν(CO) values may reflect electrostatic effects rather than the extent of Ir to CO π-back-donation.[14] They have also pointed out that comparing the electronic difference between analogous PCP- and POCOP-pincer complexes is not trivial because the influence of electron-withdrawing oxygen atoms on the phosphorus donors may be offset by the increased O→C(aryl) π-donation.[15] Nevertheless, electrochemistry studies of (^{iPr}POCOP)NiBr and (^{iPr}PCP)NiBr carried out by the Zargarian group have also suggested that the POCOP-pincer complex is more electron deficient.[16] From the steric point of view, the O-linkages in a (^{R}POCOP)M system often impose a more obtuse P—M—P angle than the related (^{R}PCP)M system, and consequently the metal center supported by a POCOP-pincer ligand is sterically more accessible.[17] This is certainly the case for nickel hydride complexes; the P—Ni—P angle of (^{tBu}POCOP)NiH[18] [166.26(3)°] has been found to be smaller than that of (^{tBu}PCP)NiH[19] [173.54(3)°]. We thus suspected that the more electrophilic and more exposed nickel center of (^{tBu}POCOP)NiH would interact with BH_3·THF more strongly than (^{tBu}PCP)NiH, allowing us to isolate the product and fully characterize it. Guided by this hypothesis, we treated a toluene solution of (^{tBu}POCOP)NiH (**1a**) with a slight excess of BH_3·THF at 0 °C, after which an immediate color change from yellow to orange was noticed. The color of the reaction mixture remained orange when warmed up to room temperature. Removal of the volatiles under vacuum did not appear to reverse the reaction either, evidenced by the persistent orange color throughout the evaporation. The ^{1}H NMR spectrum of the isolated material in C_6D_6 displays a broad quartet at −0.45 ppm with an intensity ratio of approximately 1:1:1:1, indicative of B—H coupling. The resonance integrates as four hydrogens with respect to one pincer unit. The boron resonance of the compound appears at −35.9 ppm as a quintet in ^{11}B NMR, which collapses to a singlet in ^{11}B{^{1}H} NMR. The NMR data suggest that the adduct from (^{tBu}POCOP)NiH and BH_3·THF is a typical borohydride complex.[20] Related complexes **2b** and **2c** were synthesized in good yield from hydrides **1b** and **1c**, respectively (eq 5).

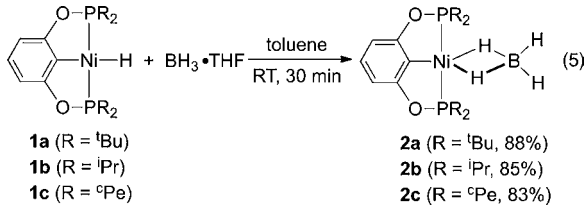

To further support the structural assignment, we prepared **2a**–**c** through an alternative route involving the displacement of Cl^- by BH_4^- from nickel chloride complexes **3a**–**c** (eq 6).

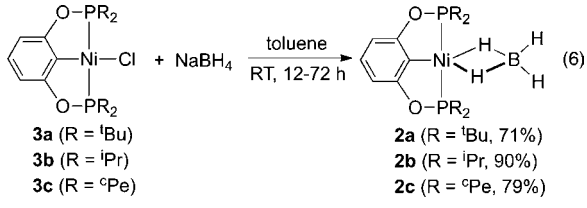

dx.doi.org/10.1021/ic300587b | Inorg. Chem. 2013, 52, 37–47

Table 1. Selected Infrared Frequencies (cm^{-1}) of 2a−c (in Solid State)[a]

	2a	2a-D_4	2b	2b-D_4	2c	2c-D_4
ν(B−H_t) or ν(B-D_t)	2412 (s)	1809 (m)	2406 (s)	1810 (m)	2387 (s)	1800 (m)
	2397 (s)	1749 (m)	2382 (s)	1753 (m)	2370 (s)	1745 (m)
		1692 (m)	2274 (w, sh)	1697 (m)		1688 (m)
ν(B−H_b) or ν(B-D_b)	1961 (br)		1947 (br)		2068 (br)	
					1886 (w)	
					1799 (br)	
BH_2 deformation			1144 (s)		1122 (s)	

[a]Abbreviations for the intensities: s, strong; m, medium; w, weak; sh, shoulder; br, broad.

The substitution reactions of **3b** and **3c** at room temperature are completed within 12 h; however, for the sterically more crowded compound **3a**, a prolonged reaction time of 3 days is needed. In any case, the NMR spectra of the product are identical to those obtained from the hydride route. The success of both synthetic methods implies that the POCOP-pincer nickel borohydride complexes are thermally stable. At room temperature, they can survive vacuum conditions for at least 24 h, and remarkably, both solid and solution samples of these complexes can be handled in air without noticeable decomposition. In strong contrast, the reaction of (^{tBu}PCP)-NiCl with $NaBH_4$ have been previously shown to generate (^{tBu}PCP)NiH as the isolable product,[21] with (^{tBu}PCP)Ni(BH_4) being the transient intermediate that is only observed in solution by NMR spectroscopy.[8] As discussed earlier, the PCP-pincer system bears a less electrophilic and sterically more crowded nickel center, therefore disfavoring the formation of the borohydride complexes.

The coordination mode of BH_4^- was first established by IR spectroscopy. Attenuated total reflectance IR spectra of the solid samples of **2a−c** show two strong bands within the range of 2370−2420 cm^{-1}, which are attributed to terminal hydrogen−boron stretch [ν(B−H_t)]. The bridging boron−hydrogen stretching bands [ν(B−H_b)] are very broad but located in the region 1790−2070 cm^{-1}. Compounds **2b** and **2c** also have a strong band at 1144 cm^{-1} and 1122 cm^{-1}, respectively, which are assigned as the BH_2 deformation mode. However, such a band is absent in **2a**, or more likely obscured by the bands associated with the pincer framework. The IR spectra of deuterium-labeled **2a−c** (synthesized from **3a−c** and $NaBD_4$) exhibit the predicted terminal deuterium-boron stretching bands from the known ν(B−H)/ν(B-D) ratio of around 1.35.[22] All these data, as summarized in Table 1, are consistent with transition metal complexes bearing a bidentate or η^2-BH_4^- ligand.[20,23] Transmission-IR spectra of **2a−c** in CH_2Cl_2 reproduce the major IR features with bands being slightly shifted from those observed for the solid samples, suggesting that the η^2-coordination mode is also the ground-state structure in solution. The magnetic equivalence of terminal and bridging hydrogens observed in the ^{1}H NMR spectra does suggest that these hydrogens are rapidly exchanged on the NMR time scale, possibly through an intermediate involving an η^1- or η^3-BH_4.

Among the known nickel borohydride complexes, very few have been characterized by X-ray crystallography.[24−28] The BH_4^- ligand in both *trans*-NiH(BH_4)(PCy_3)$_2$[24] [Cy = cyclohexyl] and (triphos)Ni(BH_4)[26] [triphos = MeC(CH_2PPh_2)$_3$] coordinates to nickel in an η^2 fashion, whereas the same ligand in Tp*Ni(BH_4)[25] [Tp* = hydrotris(3,5-dimethylpyrazolyl)-borate] adopts an η^3 coordination mode. A recent study of Ni(cyclam)(BH_4)$_2$ [cyclam = 1,4,8,11-tetraazacyclotetradecane] has shown two isomeric structures: one contains two *trans* η^1-BH_4 ligands, while the other isomer is ionic with an η^2-BH_4 ligand and a BH_4^- counterion.[27] For a dinuclear Ni(II) complex, BH_4^- bridges two nickel centers as a $\mu_{1,3}$ ligand.[28] In our case, X-ray structure determination of **2a−c** reveals an η^2-BH_4 ligand (Figures 2−4), which is consistent with the IR

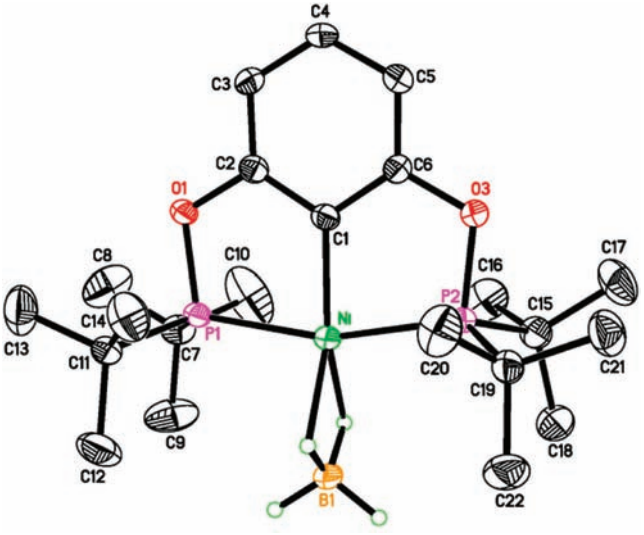

Figure 2. ORTEP drawing of [2,6-(^{t}Bu$_2$PO)$_2$C$_6$H$_3$]Ni(η^2-BH_4) (**2a**) at the 50% probability level. Hydrogen atoms except those attached to boron are omitted for clarity.

studies described above. As shown in Table 2, the B−H lengths and H−B−H angles agree with a tetrahedral geometry for the boron, when factored in with relatively large errors in locating the positions of hydrogen atoms by X-ray diffraction. Compared to the reported Ni−H length of 1.37(3) Å for **1a**,[18] the Ni−H lengths in **2a** [1.78(3) Å and 1.85(3) Å] are substantially elongated. The Ni···B distances in **2a−c** [2.180(3)−2.214(3) Å] are similar to those in *trans*-NiH(η^2-BH_4)(PCy_3)$_2$[24] [2.201(8) Å], (triphos)Ni(η^2-BH_4)[26] [2.24 Å] and [Ni(cyclam)(η^2-BH_4)]$^+$[BH_4]$^-$ [2.202(6) Å],[27] but significantly longer than those in Tp*Ni(η^3-BH_4) [2.048(5) Å][25] as well as Mindiola's PNP-pincer nickel boryl complex [1.9091(18) Å].[9b]

Loss of BH_3 from Nickel Borohydride Complexes. Although **2a−c** are incredibly robust at ambient conditions, they do lose BH_3 under forcing conditions, particularly in the case of **2a** with a relatively crowded nickel center. For instance, heating a solid sample of **2a** under a dynamic vacuum at 60 °C for 24 h produces **1a** with a 17% conversion. In contrast, **2b** and **2c** remain intact under the same conditions. An alternative

dx.doi.org/10.1021/ic300587b | Inorg. Chem. 2013, 52, 37−47

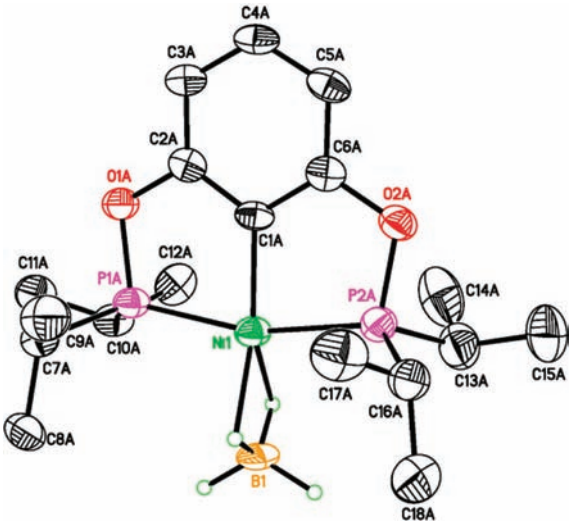

Figure 3. ORTEP drawing of [2,6-(^{i}Pr$_2$PO)$_2$C$_6$H$_3$]Ni(η^2-BH$_4$) (**2b**) at the 50% probability level. Hydrogen atoms except those attached to boron are omitted for clarity. (Two independent molecules were found in the crystalline lattice; only one is shown here).

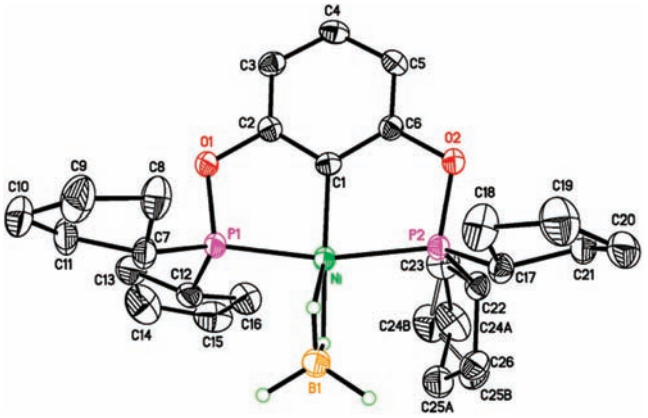

Figure 4. ORTEP drawing of [2,6-(^{c}Pe$_2$PO)$_2$C$_6$H$_3$]Ni(η^2-BH$_4$) (**2c**) at the 50% probability level. Hydrogen atoms except those attached to boron are omitted for clarity (One of the cyclopentyl rings shows some disorder; a two-component model is presented for C24/C25 with 55% major occupancy).

way to exclude BH_3 from a borohydride complex is by adding NEt_3 to form a stable BH_3·NEt_3 adduct (eq 7).

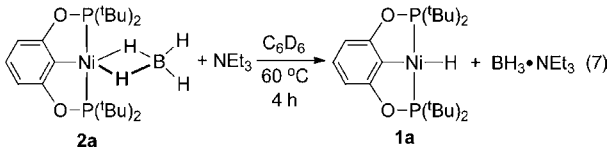

Such a reaction with **2a** at 60 °C yields **1a** cleanly and nearly quantitatively within 4 h. The decomplexation of BH_3 from **2b** and **2c**, on the other hand, are much more sluggish. After 24 h at 60 °C, approximately 40% of **2b** and **2c** are converted to the corresponding nickel hydride complexes. In addition, side products start to form, as indicated by $^{31}P\{^{1}H\}$ NMR spectroscopy; however, identifying these species is impossible because of their instability and the complexity of the NMR spectra. Our previous work on related pincer complexes has suggested that the P–O bonds are vulnerable to attack by a base, resulting in breakdown of the pincer backbone.[29]

Table 2. Selected Bond Lengths (Å) and Angles (deg)[a]

	2a	2b (A)	2b (B)	2c
Ni–H$_b$	1.78(3)	1.77(4)	1.78(5)	1.60(3)
	1.85(3)	1.87(4)	1.87(5)	1.86(3)
B1–H$_b$	1.17(3)	1.10(5)	1.15(5)	1.14(3)
	1.22(3)	1.19(5)	1.15(5)	1.28(3)
B1–H$_t$	1.04(3)	1.11(5)	1.13(5)	1.12(3)
	1.06(3)	1.16(5)	1.16(5)	1.17(3)
Ni–C1	1.901(2)	1.898(4)	1.900(4)	1.892(2)
Ni–P1	2.2046(7)	2.1514(13)	2.1643(13)	2.1475(6)
Ni–P2	2.2025(7)	2.1490(13)	2.1581(13)	2.1473(6)
Ni···B1	2.214(3)	2.187(5)	2.189(5)	2.180(3)
P1–Ni–P2	163.03(3)	163.08(5)	163.14(5)	161.49(3)
C1–Ni–P1	81.65(8)	81.28(13)	82.15(12)	81.96(7)
C1–Ni–P2	81.44(8)	81.98(13)	81.60(12)	81.84(7)
H$_b$–Ni–H$_b$	65(1)	63(2)	63(2)	67(1)
H$_b$–B–H$_b$	110(2)	113(3)	112(3)	105(2)
H$_t$–B–H$_t$	109(2)	117(3)	115(3)	113(2)

[a]Two independent molecules were found in the crystalline lattice of **2b**, which are indicated here as molecules A and B.

Evidently, the bulky ^{t}Bu groups in **2a** not only facilitate the loss of BH_3, but also shield the P–O bonds preventing potential decomposition reactions.

Reduction of CO_2 with Nickel Borohydride Complexes. Given the fact that **2a–c** can dissociate to form nickel hydrides and a borane (B_2H_6), we sought to explore the possibility of reducing CO_2 with these borohydride complexes following mechanistic steps analogous to those outlined in Scheme 1. When exposed to 1 atm of CO_2 at room temperature, none of the borohydride complexes show any reactivity. However, at 60 °C, **2a** is fully converted to a nickel formate complex **4a** over a period of 8 h (eq 8).

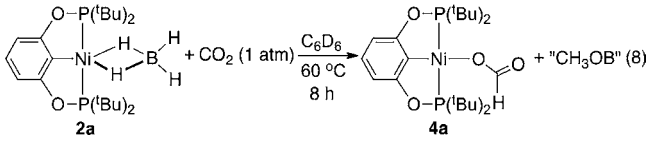

The ^{1}H NMR spectrum of the reaction mixture also reveals several resonances in the range of 3.33–3.62 ppm, suggesting that CO_2 is reduced to $(CH_3O)_3B$ and other methoxyboryl species.[30] Under the same conditions, **2b** and **2c** are much less reactive toward CO_2, producing only 5–8% of the corresponding nickel formate complexes even after 48 h. The amounts of methoxyboryl species are negligible in both cases. The results here parallel the trend observed in BH_3 decomplexation experiments as described above; a pincer ligand with smaller phosphorus substituents allows nickel to bind to BH_4^- more tightly, leading to less efficient release of BH_3 for subsequent reactions.

Reactions of Nickel Hydride Complexes with 9-BBN [9-BBN = 9-Borabicyclo(3.3.1)nonane). We have recently shown that at room temperature in the presence of 9-BBN (as a dimer), the formate moiety of **4a** can be reduced to *B*-methoxy-9-BBN.[3] Because the hydride species **1a** is cleanly produced in this process and because **1a** is known to react with CO_2 to reform **4a**, 9-BBN could be a suitable reagent for the catalytic reduction of CO_2, *only if* its interaction with **1a** does not play a detrimental role. This prompted us to investigate the reactions of nickel hydride complexes **1a–c** with 9-BBN. We first focused on the reactivity of **1a**, which shows no color change upon

dx.doi.org/10.1021/ic300587b | Inorg. Chem. 2013, 52, 37–47

mixing with a half-equivalent of 9-BBN dimer in C_6D_6. Both ^1H NMR and $^{31}P\{^1H\}$ NMR spectra of the mixture confirm no net reaction. It should be noted, however, that the deuterium in (^{tBu}POCOP)NiD exchanges readily with the BH proton of 9-BBN dimer, indicating some degree of interaction between the two species. The intermediate for this exchange process could involve any of the structures **A**–**D** shown in Figure 1.

The sterically less demanding hydride **1b** behaves drastically differently. Its yellow solution in C_6D_6 turns deep red once mixed with a half-equivalent of 9-BBN dimer. The $^{31}P\{^1H\}$ spectrum shows two resonances (both singlets) at 206.55 ppm and 200.80 ppm in a ratio of 22:78. The minor peak corresponds to the unreacted **1b** while the major one suggests a new species **5b** being formed. The most characteristic hydrogen resonance of **5b** is a broad singlet at −2.22 ppm ($\Delta\nu_{1/2}$ = 148 Hz at 22 °C), which integrates as two hydrogens per pincer molecule. Replacing the NMR solvent with toluene-d_8 allowed us to examine the reaction in a wider temperature range. From −50 to 40 °C, the ratio between **1b** and **5b** is nearly invariant but the hydride resonance of **5b** becomes much sharper at lower temperature. Above 40 °C, both hydride and phosphorus resonances of **1b** and **5b** are significantly broadened and eventually coalesce at about 70 °C. The room-temperature ^{11}B NMR spectrum shows a singlet at 27.8 ppm for the unreacted 9-BBN[31] and a singlet at −10.9 ppm presumably for **5b**. The negative chemical shift is consistent with a four-coordinate boron center,[32] and **5b** is thus best described as a dihydridoborate complex. The coordination mode of the dihydridoborate ligand is likely to be η^2, because the IR spectrum of the reaction mixture in toluene shows no bands in the $\nu(B-H_t)$ region. Such a coordination mode for $[H_2$-9-BBN$]^-$ has also been commonly observed in other transition metal systems.[7c–f,10b,32b,33] The fact that **1b**, **5b**, and 9-BBN coexist in solution with no change in ratios over time suggests that the reaction is under an equilibrium condition (eq 9).

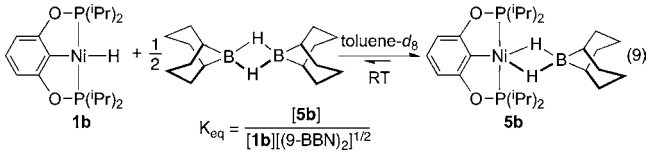

The K_{eq} value at 22 °C was determined to be 13.1 ± 4.5 $M^{-1/2}$ from $^{31}P\{^1H\}$ NMR integrations and the initial concentrations of **1b** and 9-BBN.[34] The entropy loss due to the formation of the adduct **5b** is presumably compensated by the entropy gained from the dissociation of 9-BBN dimer, which explains the virtual insensitivity of the equilibrium constant toward temperature change.

We reasoned, based on steric grounds, that **1c** might have a slight advantage over **1b** in promoting the formation of the related dihydridoborate complex. Indeed, the reaction of **1c** with 9-BBN in toluene-d_8 generates **5c** as the major species with only 5% (based on $^{31}P\{^1H\}$ NMR) of unreacted **1c**. The hydride resonance of **5c** appears at −1.87 ppm as a broad singlet ($\Delta\nu_{1/2}$ = 107 Hz at 22 °C) and the phosphorus and boron resonances are found at 187.72 ppm and −11.7 ppm in $^{31}P\{^1H\}$ and ^{11}B NMR spectra, respectively. One interesting observation made during the reaction of **1c**, however, was that after several hours, a small amount (<5%) of a second new species was produced, as first suggested by a proton resonance centered at 4.14 ppm as a doublet of doublet of triplets (J = 323.6, 15.2, and 3.6 Hz). The amount of this new species did not increase appreciably over a period of 36 h, and the unreacted **1c** remained present in the solution. On the basis of the large one-bond coupling constant of 323.6 Hz and the splitting pattern, we hypothesized that 9-BBN could also attack the more exposed pincer backbone to release (^{c}Pe)$_2$PH from the nickel pincer complex as a borane adduct (^{c}Pe)$_2$PH·(9-BBN). This was confirmed by examining the ^1H NMR spectrum of the 2:1 mixture of (^{c}Pe)$_2$PH and 9-BBN dimer in toluene-d_8. In addition, this adduct exhibits a ^{31}P resonance at −6.80 ppm and a ^{11}B resonance at −18.1 ppm, both of which are present in the corresponding NMR spectra of the **1c**/9-BBN reaction. Despite the complexity due to the side reaction as well as the unreacted hydride **1c**, the IR spectrum of the reaction mixture in toluene clearly indicates no $\nu(B-H_t)$ bands. Therefore, the dihydridoborate ligand in the major species **5c** is expected to adopt an η^2-coordination mode, in a similar fashion as the BH_4^- ligand in **2a**–**c**.

Fortunately, X-ray quality single crystals were successfully grown from a toluene solution of **5c** (generated in situ) layered with pentane at −30 °C. When the crystals were left dry, their deep red color faded immediately to yellow, implying the formation of the nickel hydride **1c** owing to the dissociation of 9-BBN. Extra care was thus taken to ensure that the crystals made contact with a small amount of mother liquid, and then were quickly covered with Paratone oil prior to X-ray diffraction at low temperature (−123 °C). To our knowledge, **5c** is the first crystallographically characterized nickel 9-BBN complex. As shown in Figure 5, dihydridoborate acts as a bidentate ligand. The Ni···B distance of 2.207(3) Å is comparable to those in **2a**–**c**, but much longer than the sum of Ni and B covalent radii of 2.08 Å.[35] Disregarding the ^{c}Pe groups, the structure would belong to a C_{2v} point group. The deviation from planarity for the plane generated by P1, C1, P2, Ni, B1, C27, and C31 atoms is only 0.0171 Å. If Y is defined as

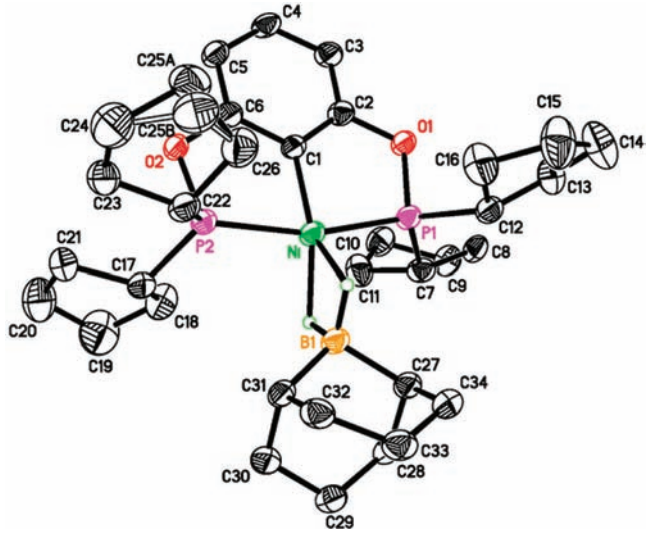

Figure 5. ORTEP drawing of [2,6-(^{c}Pe$_2$PO)$_2$C$_6$H$_3$]Ni(μ-H)$_2$[B-(C$_8$H$_{14}$)] (**5c**) at the 50% probability level. Hydrogen atoms except those attached to boron are omitted for clarity (One of the cyclopentyl rings shows some disorder; a two-component model is presented for C25 with 70% major occupancy). Selected bond lengths (Å) and angles (deg): Ni–H 1.71 (3) and 1.77 (2), B1–H both 1.20 (3), Ni–C1 1.901(2), Ni–P1 2.1570(8), Ni–P2 2.1586(8), Ni···B1 2.207(3), P1–Ni–P2 163.33(3), C1–Ni–P1 81.41(8), C1–Ni–P2 81.96(8), H–Ni–H 65(1), H–B–H 104(2).

dx.doi.org/10.1021/ic300587b | Inorg. Chem. 2013, 52, 37–47

the centroid of C27 and C31 atoms, it is almost linear with Ni and B1 with a Ni−B1−Y angle of 179.48°. These structural parameters provide further evidence supporting the η^2-coordination mode.

Reactivities of Nickel Dihydridoborate Complex 5c. At room temperature, a complete conversion from **5c** to **1c** is accomplished under a dynamic vacuum in just 1 h. The use of any reagents that trap either 9-BBN or **1c** should also perturb the equilibrium (similar as the one in eq 9). As predicted, addition of 1 equiv of NEt_3 to a solution of **5c** in C_6D_6 produces **1c** and 9-BBN·NEt_3 in 90% conversion (Scheme 2).

Scheme 2

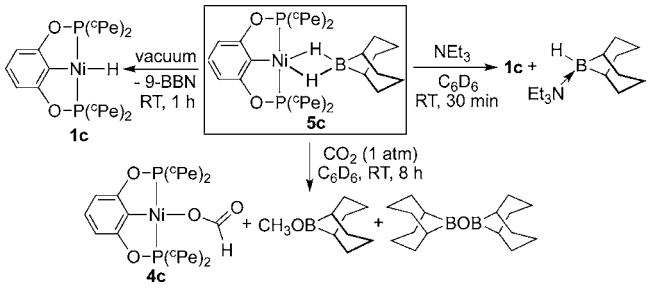

Additionally, **5c** readily reacts with CO_2 (~1 atm), as suggested by an immediate color change from red to yellow. In view of rapid insertion of CO_2 into **1c**, the obtained nickel species was initially postulated as the insertion product, nickel formate complex **4c**. However, the ^{1}H NMR spectrum of the reaction mixture shows a new peak at 8.62 ppm, which is shifted from 8.39 ppm for the formate resonance of **4c**. The $^{31}P\{^1H\}$ NMR spectrum also displays a more downfield shifted resonance (175.24 ppm) than the one for **4c** (173.35 ppm). Perhaps the new species is an adduct of **4c** and 9-BBN through a Lewis acid−base interaction. An alternative structure involving both a hydride and a formate bridging nickel and boron centers cannot be ruled out. In any event, **4c** slowly forms over a period of 8 h, with a concurrent formation of *B*-methoxy-9-BBN and a borate ester (Scheme 2).

Reactions of Nickel Hydride Complexes with HBcat. Catecholborane (HBcat) was the borane of choice when we conducted our initial investigation of reduction (or hydroboration) of CO_2 catalyzed by **1a**.[1] Compared to BH_3 and 9-BBN, HBcat has a less electrophilic boron center because of the donation of electrons from neighboring oxygen atoms. As a result, it is less favorable for HBcat to abstract H^- from a nickel hydride complex to produce a dihydridoborate complex. When a solution of **1a** in C_6D_6 was treated with 1 equiv of HBcat at room temperature, no color change was observed. Judging from the $^{31}P\{^1H\}$ and ^{11}B NMR spectra, there is no net reaction between the two species. However, the ^{1}H NMR spectrum reveals the absence of NiH and BH resonances, suggesting a rapid exchange process involving these two hydrogens. All other resonances of **1a** and HBcat remain the same as those for individual reagents. Variable-temperature (from −50 °C to +60 °C) experiments in toluene-d_8 show negligible difference in the ^{1}H NMR spectra.[36] Similarly, the mixture of (^{tBu}POCOP)NiD and HBcat (approximately 1: 1) in C_6D_6 shows no resonance in the hydride region. It is interesting to note that the $^{31}P\{^1H\}$ NMR spectrum resembles **1a** rather than (^{tBu}POCOP)NiD. These two species are distinguishable because the ^{31}P resonance of **1a** appears at 219.35 ppm as a singlet while the ^{31}P resonance of (^{tBu}POCOP)NiD exhibits at 219.39 ppm as a 1: 1: 1 triplet due to isotope shift and $^{31}P-^2H$ coupling. Evaporation of the volatiles[37] under vacuum followed by redissolution of the residue in C_6D_6 shows 88% of the nickel species containing protium on the metal, which further supports the exchange of hydrogens between **1a** and HBcat. The fact that protium concentrates at the nickel center rather than the boron center probably reflects an equilibrium isotope effect, which is often generalized by the statement "deuterium prefers the stronger bond".[38] The B−H bond dissociation energy (BDE) of HBcat has been previously calculated as 111 kcal/mol[39] whereas the BDE of a metal−hydrogen bond is typically within the range of 55−80 kcal/mol.[40]

The first sign indicating a net reaction between **1b** and HBcat was the change of color from yellow to orange when 1 equiv of HBcat was added to the solution of **1b** in C_6D_6. Although the $^{31}P\{^1H\}$ NMR spectrum only shows the resonance of **1b**, the ^{1}H NMR spectrum contains a slightly broad peak at −1.90 ppm ($\Delta\nu_{1/2}$ = 28 Hz at 22 °C), a chemical shift similar to the one observed in the **1b**/9-BBN reaction. More interestingly, this hydride resonance (for the same reaction in toluene-d_8) shifts downfield and becomes broader as the temperature decreases (Figure 6). This can be explained by an equilibrium (eq 10) that is fast on the NMR time scale.

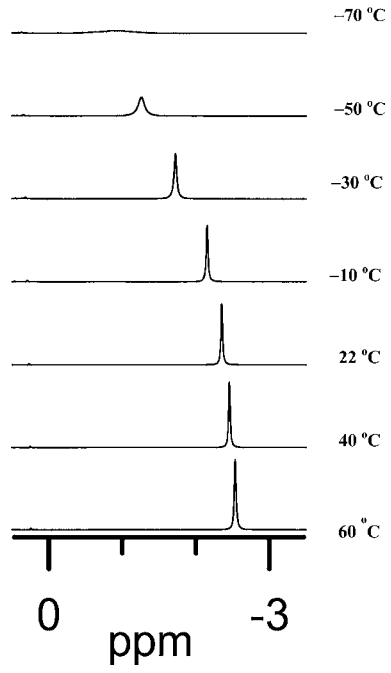

Figure 6. Variable-temperature ^{1}H NMR spectra of the 1:1 mixture of **1b** and HBcat in toluene-d_8.

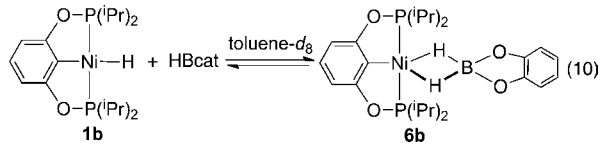

The lower temperature shifts the equilibrium more to the **6b** side, resulting in a significant change in chemical shift. The line broadening reflects the decreased rates of the forward and backward reactions; however, it is understood that even at −70 °C the reaction remains very fast. Variable-temperature

dx.doi.org/10.1021/ic300587b | Inorg. Chem. 2013, 52, 37−47

^{11}B NMR experiments provide additional evidence supporting the proposed equilibrium. At room temperature, only one resonance is observed at 27.9 ppm, which corresponds to HBcat. At −60 °C, a broad new resonance presumably for **6b** emerges at 13.7 ppm while the ^{11}B resonance of HBcat is substantially broadened and its intensity is diminished (see Supporting Information). The upfield shifted ^{11}B resonance is more consistent with a dihydridoborate complex. In contrast, the ^{11}B resonance of a σ-borane complex[4] or a metal boryl complex[6,9] is typically downfield from that of free borane.

Analogously, **1c** and HBcat are in rapid equilibrium with a dihydridoborate complex. The NMR data are similar to those described above for **1b**, except that more side reactions occur in this case. A small amount of H_2 was detected by ^{1}H NMR spectroscopy, implying that a reaction related to eq 2 is perhaps involved. In addition, a set of broad multiplets in the 3.8−5.0 ppm range is likely due to the formation of $(^cPe)_2PH{\cdot}HBcat$. ^{11}B NMR spectroscopy also reveals peaks at 22.3 ppm and 14.7 ppm, which are assigned to $B_2(cat)_3$ and $[B(cat)_2]^-$ based on literature values.[10a] Collectively, these results once again highlight the vulnerability of the P−O bonds in the presence of a hydride donor if they are not sterically protected.

Catalytic Reduction of CO_2 with Different Boranes. The aforementioned reactions of nickel hydride complexes with boranes are expected to have important implications for the catalytic reduction of CO_2. To elucidate their relationships, the catalytic performance of different combinations of nickel catalysts and boranes was investigated. In a typical catalytic reaction (eq 11), a mixture of HBR'_2 to hydride (in a 100:1 ratio) in C_6D_6 was stirred under 1 atm of CO_2 atmosphere at room temperature, and the progress of the reaction was followed by ^{1}H NMR spectroscopy.

$$CO_2\ (1\ atm) + \underset{(100\ equiv)}{3\ HBR'_2} \xrightarrow[C_6D_6,\ RT]{\text{Ni catalyst (1 equiv)}} R'_2BOCH_3 + R'_2BOBR'_2 \quad (11)$$

As shown in Table 3, no reduction of CO_2 takes place when $BH_3{\cdot}THF$ is employed as the borane source (entries 1−3).

Table 3. Catalytic Activity of Nickel Hydride Complexes in the Reduction of CO_2[a]

entry	catalyst	borane	time (h)	TON[b]
1	**1a**	$BH_3{\cdot}THF$	24	0
2	**1b**	$BH_3{\cdot}THF$	24	0
3	**1c**	$BH_3{\cdot}THF$	24	0[c]
4	**1a**	9-BBN	1	100
5	**1b**	9-BBN	1.5	100
6	**1c**	9-BBN	4	100[c]
7	**1a**	HBcat	0.75	100[d]
8	**1b**	HBcat	2	100[d]
9	**1c**	HBcat	12	30[c,d]

[a]Reaction conditions: nickel catalyst (25 μmol), borane (2.5 mmol), and hexamethylbenzene (62.5 μmol, internal standard) in 2 mL of C_6D_6 under 1 atm of CO_2 at room temperature. [b]Based on the B−H bond. [c]Hexamethyldisilane was used as the internal standard. [d]Data from ref 3.

Reactions in eq 5 suggest that the nickel catalysts would be trapped as the borohydride complexes **2a−c**. At room temperature, the release of nickel hydrides **1a−c** back to the catalytic cycles is highly unfavorable, thereby preventing the reduction of CO_2.

However, when 9-BBN is utilized as the borane source, catalytic reduction of CO_2 occurs readily under the influence of nickel hydrides **1a−c** (entries 4−6). As the size of the substituents on the phosphorus donors decreases (from **1a** to **1b** to **1c**), the required time to reach the maximum turnover number (TON) of 100 (based on the B−H bond) becomes longer. Arguably, electronic effects of the pincer ligand might also be used to rationalize the reactivity differences between these nickel hydrides. Bush and Angelici have demonstrated that ^{t}Bu-substituted phosphines are in general more basic than other alkyl-substituted phosphines.[41] If it is also true in our case with the POCOP-pincer ligand, **1a** could possess the most hydridic hydrogen among the three hydrides examined, thereby promoting the turnover-limiting insertion of boryl formate into the nickel hydride (Cycle II in Scheme 1). Nevertheless, the relative catalytic activity of the hydride complexes correlates nicely with their relative reactivity observed in the stoichiometric reaction with 9-BBN. Complex **1a**, which is the best catalyst of the series, does not form any adduct with 9-BBN. In contrast, complex **1b** reacts with 9-BBN to form a dihydridoborate complex **5b**, as demonstrated in eq 9. Although this process is reversible and the release of **1b** from **5b** is reasonably fast, the equilibrium should reduce the steady-state concentration of the active hydride species, resulting in slower catalysis. In the case of **1c**, the analogous equilibrium is even more favorable toward the catalytically dormant species **5c**. The observation of a phosphine-borane adduct $(^cPe)_2PH{\cdot}(9\text{-BBN})$ in the stoichiometric reaction suggests that the decomposition of catalyst **1c** by 9-BBN through the cleavage of P−O bonds may play an additional role in reducing the concentration of **1c** during catalysis.

Compared to 9-BBN, HBcat has a weaker interaction with the nickel hydride complexes. Related dihydridoborate complexes do form when complexes **1b** and **1c** are mixed with HBcat, but at room temperature they exist in such a small quantity that they should not drastically impact the catalysis. Experimental results (entries 7−9) show that **1b** is a less active catalyst than **1a**. More surprisingly, the reaction catalyzed by **1c** did not go to completion with a TON of only 30 after 12 h. We suspected that catalysis was plagued with severe catalyst degradation (for **1c** in particular) as described in the stoichiometric study.

CONCLUDING REMARKS

We have synthesized or spectroscopically observed nickel dihydridoborate complexes from the reactions between POCOP-pincer-ligated nickel hydrides and various boranes. The extent of formation of such complexes is not only dependent on the substituents on the phosphorus donor atoms, but also dependent on the type of boranes. We have shown that nickel hydride complexes react with $BH_3{\cdot}THF$ irreversibly at room temperature to yield BH_4-complexes, which can be considered as a special case of dihydridoborate complexes. Reversing the reactions is possible at higher temperatures if there is a trapping agent available, or under a dynamic vacuum. Other boranes such as 9-BBN and HBcat are also capable of reacting with nickel hydride complexes to form the corresponding nickel dihydridoborate complexes, unless the hydride moiety is sterically inaccessible. However, these reactions are reversible at room temperature, allowing nickel hydride species to reform under most circumstances. In the catalytic reduction of CO_2 with boranes, the dihydridoborate complexes, when they are formed, serve as dormant species

dx.doi.org/10.1021/ic300587b | Inorg. Chem. 2013, 52, 37−47

outside the catalytic cycles. The catalytic reactions are fast when the nickel catalyst contains bulky substituents on the phosphorus donor atoms. Another benefit of these bulky substituents is that they protect the P−O bonds of the pincer ligand from borane attack and thus minimize catalyst degradation.

EXPERIMENTAL SECTION

General Comments. Unless otherwise noted, all the organometallic compounds were prepared and handled under an argon atmosphere using standard Schlenk and inert-atmosphere box techniques. Dry and oxygen-free solvents (toluene and tetrahydrofuran (THF)) were collected from an Innovative Technology solvent purification system and used throughout the experiments. Benzene-d_6 and toluene-d_8 were distilled from Na and benzophenone under an argon atmosphere. Other solvents (pentane and CD_2Cl_2) were used as received from commercial sources. Catecholborane was purified by vacuum distillation prior to use, and other boranes were purchased from Sigma-Aldrich and used without further purification. ^{1}H, ^{13}C, and ^{31}P NMR spectra were recorded on a Bruker Avance-400 MHz spectrometer. ^{11}B NMR spectra were recorded on a Bruker AMX 400 MHz wide-bore spectrometer. Chemical shift values in ^{1}H and ^{13}C NMR spectra were referenced internally to the residual solvent resonances. ^{31}P and ^{11}B NMR spectra were referenced externally to 85% H_3PO_4 (0 ppm) and $BF_3{\cdot}Et_2O$ (0 ppm), respectively. Infrared spectra were recorded on a Thermo Scientific Nicolet 6700 FT-IR spectrometer equipped with smart orbit diamond attenuated total reflectance (ATR) accessory. (^{tBu}POCOP)NiH (**1a**),[18] (^{iPr}POCOP)-NiH (**1b**),[18] (^{cPe}POCOP)NiH (**1c**),[3] (^{tBu}POCOP)NiCl (**3a**),[18] (^{iPr}POCOP)NiCl (**3b**),[42] and (^{cPe}POCOP)NiCl (**3c**)[3] were prepared as described in the literature. (^{tBu}POCOP)NiD (98 atom % D) was synthesized from **3a** and $LiAlD_4$ (98 atom % D) following a procedure used for **1a**.[18]

Synthesis of (^{tBu}POCOP)Ni(BH$_4$) (2a). *Method A from 1a*: Under an argon atmosphere, a 1.0 M solution of $BH_3{\cdot}$THF in THF (0.33 mL, 0.33 mmol) was added slowly to a Schlenk flask containing a chilled solution (0 °C) of **1a** (100 mg, 0.22 mmol) in 10 mL of toluene. The color of the solution changed immediately from yellow to orange. After stirring at room temperature for 30 min, the reaction mixture was exposed to air and filtered through a pad of Celite. Removal of the volatiles under vacuum afforded an orange solid, which was further purified by washing with pentane (3 mL × 3) and then drying under vacuum (91 mg, 88% yield). *Method B from 3a*: Under an argon atmosphere, 10 mL of toluene was added to a Schlenk flask containing **3a** (100 mg, 0.20 mmol) and $NaBH_4$ (9.0 mg, 0.24 mmol). The reaction mixture was stirred at room temperature for 3 d, resulting in a yellow-orange solution, which was filtered through a pad of Celite (in air) and evaporated to dryness. The obtained orange solid was washed with pentane (3 mL × 3) and dried under vacuum to afford the pure product (68 mg, 71% yield). ^{1}H NMR (400 MHz, C_6D_6, δ): −0.45 (br q, NiBH_4, 4H), 1.37 (vt, $^3J_{H-P}$ = 7.0 Hz, CH_3, 36H), 6.56 (d, Ar$H^{3/5}$, $^3J_{H-H}$ = 8.0 Hz, 2H), 6.85 (t, ArH^4, $^3J_{H-H}$ = 8.0 Hz, 1H). ^{1}H NMR (400 MHz, CD_2Cl_2, δ): −1.13 (br q, $^1J_{H-B}$ = 80 Hz, NiBH_4, 4H), 1.43 (vt, $^3J_{H-P}$ = 7.0 Hz, CH_3, 36H), 6.41 (d, Ar$H^{3/5}$, $^3J_{H-H}$ = 8.0 Hz, 2H), 6.90 (t, ArH^4, $^3J_{H-H}$ = 8.0 Hz, 1H). ^{13}C{^{1}H} NMR (101 MHz, C_6D_6, δ): 27.95 (t, J_{C-P} = 2.7 Hz, CH_3), 40.06 (t, J_{C-P} = 7.6 Hz, PC$(CH_3)_3$), 105.14 (t, J_{C-P} = 6.1 Hz, Ar$C^{3/5}$), 169.47 (t, J_{C-P} = 8.8 Hz, Ar$C^{2/6}$); other resonances were obscured by the solvent peaks. ^{13}C{^{1}H} NMR (101 MHz, CD_2Cl_2, δ): 28.03 (s, CH_3), 40.28 (t, J_{C-P} = 7.7 Hz, PC$(CH_3)_3$), 104.86 (t, J_{C-P} = 6.1 Hz, Ar$C^{3/5}$), 127.65 (t, J_{C-P} = 20.5 Hz, ArC^1), 127.76 (s, ArC^4), 169.34 (t, J_{C-P} = 8.7 Hz, Ar$C^{2/6}$). ^{31}P{^{1}H} NMR (162 MHz, C_6D_6, δ): 200.15 (s). ^{31}P{^{1}H} NMR (162 MHz, CD_2Cl_2, δ): 200.03 (s). ^{11}B NMR (128 MHz, C_6D_6, δ): −35.9 (quin, $^1J_{B-H}$ = 65.4 Hz). ^{11}B{^{1}H} NMR (128 MHz, C_6D_6, δ): −35.9 (s). Selected data from ATR-IR (solid, cm^{-1}): 2412 (s), 2397 (s), 1961 (br). Selected data from transmission-IR (CH_2Cl_2, cm^{-1}): 2412 (s), 2397 (s), 1955 (br). Anal. Calcd for $C_{22}H_{43}O_2BP_2Ni$: C, 56.10; H, 9.20. Found: C, 55.88; H, 9.15.

(^{iPr}POCOP)Ni(BH$_4$) (2b). **2b** was prepared in 85% yield via *Method A* following procedures similar to those used for **2a**. This compound was also prepared in 90% yield via *Method B*, although the reaction time was shortened to 12 h. ^{1}H NMR (400 MHz, C_6D_6, δ): −0.71 (br q, NiBH_4, 4H), 1.05−1.10 (m, PCH(CH_3)$_2$, 12H), 1.23−1.29 (m, PCH(CH_3)$_2$, 12H), 2.07−2.14 (m, PCH(CH$_3$)$_2$, 4H), 6.61 (d, Ar$H^{3/5}$, $^3J_{H-H}$ = 8.0 Hz, 2H), 6.85 (t, ArH^4, $^3J_{H-H}$ = 8.0 Hz, 1H). ^{1}H NMR (400 MHz, CD_2Cl_2, δ): −1.39 (br q, $^1J_{H-B}$ = 79 Hz, NiBH_4, 4H), 1.24−1.36 (m, PCH(CH_3)$_2$, 24H), 2.29−2.36 (m, PCH(CH$_3$)$_2$, 4H), 6.42 (d, Ar$H^{3/5}$, $^3J_{H-H}$ = 8.0 Hz, 2H), 6.91 (t, ArH^4, $^3J_{H-H}$ = 8.0 Hz, 1H). ^{13}C{^{1}H} NMR (101 MHz, C_6D_6, δ): 16.60 (s, CH_3), 16.89 (s, CH_3), 28.35 (t, J_{C-P} = 11.9 Hz, PCH), 105.49 (t, J_{C-P} = 6.4 Hz, Ar$C^{3/5}$), 168.75 (t, J_{C-P} = 9.6 Hz, Ar$C^{2/6}$); other resonances were obscured by the solvent peaks. ^{13}C{^{1}H} NMR (101 MHz, CD_2Cl_2, δ): 16.74 (CH_3), 16.99 (t, J_{C-P} = 2.5 Hz, CH_3), 28.49 (t, J_{C-P} = 11.9 Hz, PC$(CH_3)_3$), 105.18 (t, J_{C-P} = 6.5 Hz, Ar$C^{3/5}$), 127.92 (s, ArC^4), 129.78 (t, J_{C-P} = 21.3 Hz, ArC^1), 168.52 (t, J_{C-P} = 9.5 Hz, Ar$C^{2/6}$). ^{31}P{^{1}H} NMR (162 MHz, C_6D_6, δ): 199.43 (s). ^{31}P{^{1}H} NMR (162 MHz, CD_2Cl_2, δ): 199.28 (s). ^{11}B NMR (128 MHz, C_6D_6, δ): −33.5 (quin, $^1J_{B-H}$ = 63.9 Hz). ^{11}B{^{1}H} NMR (128 MHz, C_6D_6, δ): −33.5 (s). Selected data from ATR-IR (solid, cm^{-1}): 2406 (s), 2382 (s), 2274 (w), 1947 (br), 1144 (s). Selected data from transmission-IR (CH_2Cl_2, cm^{-1}): 2398 (s), 2380 (s), 2273 (w), 1954 (br), 1143 (s). Anal. Calcd for $C_{18}H_{35}O_2BP_2Ni$: C, 52.10; H, 8.50. Found: C, 52.30; H, 8.47.

(^{cPe}POCOP)Ni(BH$_4$) (2c). **2c** was prepared in 83% yield (via *Method A*) and 79% yield (via *Method B*) by procedures similar to those used for **2b**. ^{1}H NMR (400 MHz, C_6D_6, δ): −0.63 (br d, NiBH_4, 4H), 1.37−2.10 (m, CH_2, 32H), 2.34−2.38 (m, PCH, 4H), 6.64 (d, Ar$H^{3/5}$, $^3J_{H-H}$ = 7.2 Hz, 2H), 6.87 (t, ArH^4, $^3J_{H-H}$ = 7.2 Hz, 1H). ^{1}H NMR (400 MHz, CD_2Cl_2, δ): −1.39 (br q, NiBH_4, 4H), 1.61−1.77 (m, CH_2, 32H), 2.41−2.46 (m, PCH, 4H), 6.39 (d, Ar$H^{3/5}$, $^3J_{H-H}$ = 8.0 Hz, 2H), 6.89 (t, ArH^4, $^3J_{H-H}$ = 8.0 Hz, 1H). ^{13}C{^{1}H} NMR (101 MHz, C_6D_6, δ): 26.57 (t, J_{C-P} = 4.4 Hz, CH_3), 26.99 (t, J_{C-P} = 3.6 Hz, CH_3), 27.88 (t, J_{C-P} = 3.0 Hz, CH_3), 28.32 (CH_3), 39.55 (t, J_{C-P} = 13.0 Hz, PCH), 105.58 (t, J_{C-P} = 6.5 Hz, Ar$C^{3/5}$), 130.60 (t, J_{C-P} = 21.5 Hz, ArC^1), 168.53 (t, J_{C-P} = 9.9 Hz, Ar$C^{2/6}$); one resonance was obscured by the solvent peaks. ^{13}C{^{1}H} NMR (101 MHz, CD_2Cl_2, δ): 26.67 (t, J_{C-P} = 4.5 Hz, CH_3), 27.07 (t, J_{C-P} = 3.7 Hz, CH_3), 27.85 (t, J_{C-P} = 3.2 Hz, CH_3), 28.36 (CH_3), 39.49 (t, J_{C-P} = 13.1 Hz, PCH), 105.19 (t, J_{C-P} = 6.4 Hz, Ar$C^{3/5}$), 127.80 (s, ArC^4), 130.17 (t, J_{C-P} = 21.3 Hz, ArC^1), 168.22 (t, J_{C-P} = 9.7 Hz, Ar$C^{2/6}$). ^{31}P{^{1}H} NMR (162 MHz, C_6D_6, δ): 190.42 (s). ^{31}P{^{1}H} NMR (162 MHz, CD_2Cl_2, δ): 190.43 (s). ^{11}B NMR (128 MHz, C_6D_6, δ): −32.2 (br). ^{11}B{^{1}H} NMR (128 MHz, C_6D_6, δ): −32.2 (s). Selected data from ATR-IR (solid, cm^{-1}): 2387 (s), 2370 (s), 2068 (br), 1886 (w), 1799 (br), 1122(s). Selected data from transmission-IR (CH_2Cl_2, cm^{-1}): 2381 (br s), 2075 (br), 1885 (br), 1792 (br), 1123(s). Anal. Calcd for $C_{26}H_{43}O_2BP_2Ni$: C, 60.16; H, 8.35. Found: C, 60.02; H, 8.51.

Formation of (^{cPe}POCOP)Ni(BC$_8$H$_{16}$) (5c). Under an argon atmosphere, 9-BBN dimer (13.3 mg, 54.5 μmol) and **1c** (50 mg, 99 μmol) were mixed with ∼1 mL of toluene in a scintillation vial. After standing at room temperature for 1 h, the resulting red solution was carefully layered with about the same volume of pentane and then kept in a −30 °C freezer for at least 12 h. Red crystals obtained were suitable for X-ray crystallographic study. The NMR sample was prepared by mixing a 1:2 ratio of 9-BBN dimer and **1c** in ∼0.6 mL of C_6D_6. About 5% of the total nickel species was identified as unreacted **1c**. When the solution was kept for several hours, a new species started to form and was identified as (^{c}Pe)$_2$PH·(9-BBN). Characterization data for **5c**: ^{1}H NMR (400 MHz, C_6D_6, δ): −1.80 (br s, Ni(H)$_2$B, 2H), 0.91 (br, BCH, 2H), 1.36−2.35 (m, CH and CH_2, 48H), 6.60 (d, Ar$H^{3/5}$, $^3J_{H-H}$ = 8.0 Hz, 2H), 6.83 (t, ArH^4, $^3J_{H-H}$ = 8.0 Hz, 1H). ^{31}P{^{1}H} NMR (162 MHz, C_6D_6, δ): 187.72 (s). ^{11}B NMR (128 MHz, C_6D_6, δ): −11.4 (br s). ^{11}B{^{1}H} NMR (128 MHz, C_6D_6, δ): −11.3 (s). Selected data from transmission-IR (toluene, cm^{-1}): 1943 (w), 1857 (w).

Phosphine-Borane Adduct (^{c}Pe)$_2$PH·(9-BBN) Generated in Situ. The NMR sample was prepared by mixing a 2:1 ratio of (^{c}Pe)$_2$PH and 9-BBN dimer in ∼0.6 mL of toluene-d_6. ^{1}H NMR (400 MHz, C_7D_8, δ): 1.23−2.32 (m, CH and CH_2, 32H), 4.14 (ddt, $^1J_{P-H}$ =

dx.doi.org/10.1021/ic300587b | Inorg. Chem. 2013, 52, 37−47

Table 4. Crystal Data Collection and Refinement Parameters

	2a	2b	2c	5c
empirical formula	$C_{22}H_{43}O_2BP_2Ni$	$C_{18}H_{35}O_2BP_2Ni$	$C_{26}H_{43}O_2BP_2Ni$	$C_{34}H_{55}O_2BP_2Ni$
crystal system	triclinic	monoclinic	triclinic	monoclinic
space group	$P\bar{1}$	$P2_1/c$	$P\bar{1}$	$P2_1/c$
a, Å	8.2870(2)	12.9681(4)	8.7254(1)	15.7800(7)
b, Å	12.1490(3)	23.5433(8)	10.5060(2)	13.0913(6)
c, Å	13.4267(3)	14.6846(5)	14.5596(2)	17.1942(8)
α, deg	100.274(1)	90	81.742(1)	90
β, deg	95.653(1)	100.352(1)	86.572(1)	112.518(2)
γ, deg	105.074(2)	90	83.280(1)	90
volume, Å^3	1269.32(5)	4410.4(3)	1310.50(3)	3281.2(3)
Z	2	8	2	4
no. of data collected	11009	33917	11353	22642
no. of unique data, R_{int}	4390, 0.0327	6774, 0.0987	4546, 0.0244	5826, 0.0571
R1, wR2 ($I > 2\sigma(I)$)	0.0410, 0.1045	0.0498, 0.1124	0.0389, 0.0999	0.0470, 0.1179
R1, wR2 (all data)	0.0522, 0.1119	0.0844, 0.1286	0.0452, 0.1043	0.0728, 0.1291

323.6 Hz, $^3J_{H-H}$ = 15.2 Hz, J_{H-H} = 3.6 Hz, P−*H*, 1H); B*H* was not located. $^{31}P\{^1H\}$ NMR (162 MHz, C_7D_8, δ): −6.80 (s). ^{11}B NMR (128 MHz, C_7D_8, δ): −18.1 (s).

Release of BH_3 from 2a−c under Vacuum. A solid sample of a nickel borohydride complex (25 μmol) in a J. Young NMR tube was heated at 60 °C under a dynamic vacuum for 24 h. The residue was dissolved in about 0.6 mL of benzene-d_6 for NMR analysis. The percentage conversion for each reaction was calculated by comparing the integration of the produced nickel hydride species with that of unreacted borohydride complex from the ^{31}P NMR spectrum.

Reactions of 2a−c with Triethylamine. A screw cap NMR tube was charged with a solution of a nickel borohydride complex (12 μmol) in 0.6 mL of benzene-d_6. Triethylamine (1.7 μL, 12 μmol) was added via a microliter syringe, and the NMR tube was heated by a 60 °C oil bath. The progress of the reaction was monitored by ^1H and $^{31}P\{^1H\}$ NMR spectroscopy. The percentage conversion for each reaction was calculated by comparing the integration of the produced nickel hydride species with that of unreacted borohydride complex from the ^{31}P NMR spectrum.

Reactions of 2a−c with CO_2. In a glovebox, a nickel borohydride complex (25 μmol) and 0.6 mL of benzene-d_6 were transferred into a J. Young NMR tube. The resulting solution was degassed by performing three freeze−pump−thaw cycles and then placed under 1 atm of CO_2. The NMR tube was heated by a 60 °C oil bath, and the progress of the reaction was monitored by ^1H and $^{31}P\{^1H\}$ NMR spectroscopy. The percentage conversion for each reaction was calculated by comparing the integration of the produced nickel formate complex with that of unreacted borohydride complex from the ^{31}P NMR spectrum.

Reaction of 5c with Triethylamine. In a J. Young NMR tube, complex **5c** was generated in situ by mixing **1c** (10.0 mg, 19.8 μmol) and 9-BBN dimer (2.4 mg, 9.9 μmol) in 0.6 mL of benzene-d_6 at room temperature for 1 h. To this solution, triethylamine (2.8 μL, 19.8 μmol) was added via a microliter syringe. A complete conversion to **1c** was accomplished within 30 min, as confirmed by ^1H and ^{31}P NMR spectroscopy.

Reaction of 5c with CO_2. In a J. Young NMR tube, complex **5c** was generated in situ by mixing **1c** (10.0 mg, 19.8 μmol) and 9-BBN dimer (2.4 mg, 9.9 μmol) in 0.6 mL of benzene-d_6 at room temperature for 1 h. The resulting solution was degassed by performing three freeze−pump−thaw cycles and then placed under 1 atm of CO_2. The progress of the reaction was monitored by ^1H and ^{31}P NMR spectroscopy. After 8 h, **4c** was the only nickel species observed by $^{31}P\{^1H\}$ spectroscopy. The boron-containing products were identified as the known *B*-methoxy-9-BBN[43] and a borate ester.[44]

Catalytic Reduction of CO_2 with Boranes (BH_3·THF, 9-BBN, and HBcat). Under an argon atmosphere, a flame-dried 50 mL Schlenk flask was charged with a nickel hydride complex (25 μmol), a borane (272 μL, 2.50 mmol), and 2 mL of C_6D_6. To this solution, hexamethylbenzene (10.0 mg, 62.5 μmol) was added as an internal standard except for the reactions involving **1c**. To avoid the overlap of proton resonances between hexamethylbenzene and **1c**, hexamethyldisilane was used as the internal standard. The mixture was degassed by a freeze−pump−thaw cycle and placed under 1 atm of CO_2. At different time intervals, a small portion of the clear liquid layer (ca. 0.6 mL) was withdrawn from the flask and transferred into a J. Young NMR tube under an argon atmosphere. From the ^1H NMR spectrum of the aliquot, turnover number (TON) was calculated by comparing the integration of $CH_3OBR'_2$ methyl resonance (near 3.3 ppm) with that of the internal standard (2.12 ppm).

X-ray Structure Determination. Single crystals of **2a−c** were grown from pentane at −30 °C. Single crystals of **5c** were grown from toluene-pentane at −30 °C. Crystal data collection and refinement parameters are summarized in Table 4. Intensity data were collected at 150 K on a Bruker SMART6000 CCD diffractometer using graphite-monochromated Cu Kα radiation, λ = 1.54178 Å. The data frames were processed using the program SAINT. The data were corrected for decay, Lorentz, and polarization effects as well as absorption and beam corrections based on the multiscan technique. The structures were solved by a combination of direct methods in SHELXTL and the difference Fourier technique and refined by full-matrix least-squares procedures. Non-hydrogen atoms were refined with anisotropic displacement parameters. H-atoms attached to the boron were located directly from the difference map, and their positions refined. All remaining H-atom positions were calculated and treated with a riding model. None of the structures has solvent present in the crystalline lattice. The cyclopentyl rings in **2c** and **5c** show typical disorder; a two-component model is presented for C24/C25 in **2c** (major occupancy is 55%) and C25 in **5c** (major occupancy is 70%). Compound **2b** crystallized as two independent molecules in the crystalline lattice.

■ ASSOCIATED CONTENT

Ⓢ Supporting Information

X-ray crystallographic data in CIF format and NMR data in PDF format. This material is available free of charge via the Internet at http://pubs.acs.org.

■ AUTHOR INFORMATION

Corresponding Author

*E-mail: hairong.guan@uc.edu.

Notes

The authors declare no competing financial interest.

dx.doi.org/10.1021/ic300587b | *Inorg. Chem.* 2013, 52, 37−47

■ ACKNOWLEDGMENTS

We thank the National Science Foundation (CHE-0952083) and the donors of the American Chemical Society Petroleum Research Fund (49646-DNI3) for support of this research. We are also grateful to Dr. Keyang Ding for his assistance with NMR experiments. S.C. thanks the University of Cincinnati Sigma Xi Chapter for a Grants-in-Aid of Research award. X-ray data were collected on a Bruker SMART6000 diffractometer which was funded through an NSF-MRI grant (CHE-0215950).

■ REFERENCES

(1) Chakraborty, S.; Zhang, J.; Krause, J. A.; Guan, H. *J. Am. Chem. Soc.* **2010**, *132*, 8872−8873.
(2) Huang, F.; Zhang, C.; Jiang, J.; Wang, Z.-X.; Guan, H. *Inorg. Chem.* **2011**, *50*, 3816−3825.
(3) Chakraborty, S.; Patel, Y. J.; Krause, J. A.; Guan, H. *Polyhedron* **2012**, *32*, 30−34.
(4) (a) Lachaize, S.; Essalah, K.; Montiel-Palma, V.; Vendier, L.; Chaudret, B.; Barthelat, J.-C.; Sabo-Etienne, S. *Organometallics* **2005**, *24*, 2935−2943. (b) Denney, M. C.; Pons, V.; Hebden, T. J.; Heinekey, D. M.; Goldberg, K. I. *J. Am. Chem. Soc.* **2006**, *128*, 12048−12049. (c) Hebden, T. J.; Denney, M. C.; Pons, V.; Piccoli, P. M. B.; Koetzle, T. F.; Schultz, A. J.; Kaminsky, W.; Goldberg, K. I.; Heinekey, D. M. *J. Am. Chem. Soc.* **2008**, *130*, 10812−10820.
(5) For recent reviews on σ-borane complexes, see: (a) Alcaraz, G.; Sabo-Etienne, S. *Coord. Chem. Rev.* **2008**, *252*, 2395−2409. (b) Lin, Z. *Struct. Bonding (Berlin)* **2008**, *130*, 123−148.
(6) (a) Baker, R. T.; Ovenall, D. W.; Calabrese, J. C.; Westcott, S. A.; Taylor, N. J.; Williams, I. D.; Marder, T. B. *J. Am. Chem. Soc.* **1990**, *112*, 9399−9400. (b) Hartwig, J. F.; De Gala, S. R. *J. Am. Chem. Soc.* **1994**, *116*, 3661−3662. (c) Lantero, D. R.; Motry, D. H.; Ward, D. L.; Smith, M. R., III. *J. Am. Chem. Soc.* **1994**, *116*, 10811−10812. (d) Lantero, D. R.; Miller, S. L.; Cho, J.-Y.; Ward, D. L.; Smith, M. R., III. *Organometallics* **1999**, *18*, 235−247. (e) Ohki, Y.; Hatanaka, T.; Tatsumi, K. *J. Am. Chem. Soc.* **2008**, *130*, 17174−17186.
(7) (a) Lantero, D. R.; Ward, D. L.; Smith, M. R., III. *J. Am. Chem. Soc.* **1997**, *119*, 9699−9708. (b) Hascall, T.; Bridgewater, B. M.; Parkin, G. *Polyhedron* **2000**, *19*, 1063−1066. (c) Antiñolo, A.; Carrillo-Hermosilla, F.; Fernández-Baeza, J.; García-Yuste, S.; Otero, A.; Rodríguez, A. M.; Sánchez-Prada, J.; Villaseñor, E.; Gelabert, R.; Moreno, M.; Lluch, J. M.; Lledós, A. *Organometallics* **2000**, *19*, 3654−3663. (d) Liu, X.-Y.; Bouherour, S.; Jacobsen, H.; Schmalle, H. W.; Berke, H. *Inorg. Chim. Acta* **2002**, *330*, 250−267. (e) Essalah, K.; Barthelat, J.-C.; Montiel, V.; Lachaize, S.; Donnadieu, B.; Chaudret, B.; Sabo-Etienne, S. *J. Organomet. Chem.* **2003**, *680*, 182−187. (f) Evans, W. J.; Lorenz, S. E.; Ziller, J. W. *Chem. Commun.* **2007**, 4662−4664. (g) Bontemps, S.; Vendier, L.; Sabo-Etienne, S. *Angew. Chem., Int. Ed.* **2012**, *51*, 1671−1674.
(8) Rossin, A.; Peruzzini, M.; Zanobini, F. *Dalton Trans.* **2011**, *40*, 4447−4452.
(9) (a) Burgess, K.; van der Donk, W. A.; Westcott, S. A.; Marder, T. B.; Baker, R. T.; Calabrese, J. C. *J. Am. Chem. Soc.* **1992**, *114*, 9350−9359. (b) Adhikari, D.; Huffman, J. C.; Mindiola, D. J. *Chem. Commun.* **2007**, 4489−4491. (c) Zhu, Y.; Chen, C.-H.; Fafard, C. M.; Foxman, B. M.; Ozerov, O. V. *Inorg. Chem.* **2011**, *50*, 7980−7987.
(10) (a) Westcott, S. A.; Blom, H. P.; Marder, T. B.; Baker, R. T.; Calabrese, J. C. *Inorg. Chem.* **1993**, *32*, 2175−2182. (b) Westcott, S. A.; Marder, T. B.; Baker, R. T.; Harlow, R. L.; Calabrese, J. C.; Lam, K. C.; Lin, Z. *Polyhedron* **2004**, *32*, 2665−2677. (c) Knizek, J.; Nöth, H. *Eur. J. Inorg. Chem.* **2011**, 1888−1900.
(11) Göttker-Schnetmann, I.; White, P. S.; Brookhart, M. *Organometallics* **2004**, *23*, 1766−1776.
(12) Krogh-Jespersen, K.; Czerw, M.; Zhu, K.; Singh, B.; Kanzelberger, M.; Darji, N.; Achord, P. D.; Renkema, K. B.; Goldman, A. S. *J. Am. Chem. Soc.* **2002**, *124*, 10797−10809.
(13) Kuklin, S. A.; Sheloumov, A. M.; Dolgushin, F. M.; Ezernitskaya, M. G.; Peregudov, A. S.; Petrovskii, P. V.; Koridze, A. A. *Organometallics* **2006**, *25*, 5466−5476.
(14) Goldman, A. S.; Krogh-Jespersen, K. *J. Am. Chem. Soc.* **1996**, *118*, 12159−12166.
(15) Zhu, K.; Achord, P. D.; Zhang, X.; Krogh-Jespersen, K.; Goldman, A. S. *J. Am. Chem. Soc.* **2004**, *126*, 13044−13053.
(16) (a) Pandarus, V.; Zargarian, D. *Chem. Commun.* **2007**, 978−980. (b) Castonguay, A.; Spasyuk, D. M.; Madern, N.; Beauchamp, A. L.; Zargarian, D. *Organometallics* **2009**, *28*, 2134−2141.
(17) Choi, J.; MacArthur, A. H. R.; Brookhart, M.; Goldman, A. S. *Chem. Rev.* **2011**, *111*, 1761−1779.
(18) Chakraborty, S.; Krause, J. A.; Guan, H. *Organometallics* **2009**, *28*, 582−586.
(19) Boro, B. J.; Duesler, E. N.; Goldberg, K. I.; Kemp, R. A. *Inorg. Chem.* **2009**, *48*, 5081−5087.
(20) Marks, T. J.; Kolb, J. R. *Chem. Rev.* **1977**, *77*, 263−293.
(21) Moulton, C. J.; Shaw, B. L. *J. Chem. Soc., Dalton Trans.* **1976**, 1020−1024.
(22) Corey, E. J.; Cooper, N. J.; Canning, W. M.; Lipscomb, W. N.; Koetzle, T. F. *Inorg. Chem.* **1982**, *21*, 192−199.
(23) Besora, M.; Lledós, A. *Struct. Bonding (Berlin)* **2008**, *130*, 149−202.
(24) Saito, T.; Nakajima, M.; Kobayashi, A.; Sasaki, Y. *J. Chem. Soc., Dalton Trans.* **1978**, 482−485.
(25) Desrochers, P. J.; LeLievre, S.; Johnson, R. J.; Lamb, B. T.; Phelps, A. L.; Cordes, A. W.; Gu, W.; Cramer, S. P. *Inorg. Chem.* **2003**, *42*, 7945−7950.
(26) Kandiah, M.; McGrady, G. S.; Decken, A.; Sirsch, P. *Inorg. Chem.* **2005**, *44*, 8650−8652.
(27) Churchard, A. J.; Cyranski, M. K.; Dobrzycki, L.; Budzianowski, A.; Grochala, W. *Energy Environ. Sci.* **2010**, *3*, 1973−1978.
(28) Journaux, Y.; Lozan, V.; Klingele, J.; Kersting, B. *Chem. Commun.* **2006**, 83−84.
(29) Zhang, J.; Medley, C. M.; Krause, J. A.; Guan, H. *Organometallics* **2010**, *29*, 6393−6401.
(30) Other methoxyboryl species could be $(CH_3O)_2BH$, $(CH_3OBH_3)BH(OCH_3)$, $(CH_3OBH_3)_2BOCH_3$, and $(CH_3OBH_2)_x$. For discussions, see: Burg, A. B.; Schlesinger, H. I. *J. Am. Chem. Soc.* **1933**, *55*, 4020−4025.
(31) (a) Contreras, R.; Wrackmeyer, B. *Z. Naturforsch., B* **1980**, *35*, 1236−1240. (b) Chen, X.; Liu, S.; Plečnik, C. E.; Liu, F.-C.; Fraenkel, G.; Shore, S. G. *Organometallics* **2003**, *22*, 275−283.
(32) (a) Hubbard, J. L.; Kramer, G. W. *J. Organomet. Chem.* **1978**, *156*, 81−94. (b) Chen, X.; Lim, S.; Plečnik, C. E.; Liu, S.; Du, B.; Meyers, E. A.; Shore, S. G. *Inorg. Chem.* **2004**, *43*, 692−698. (c) Barrett, A. G. M.; Crimmin, M. R.; Hill, M. S.; Hitchcock, P. B.; Procopiou, P. A. *Organometallics* **2007**, *26*, 4076−4079. (d) Spielmann, J.; Harder, S. *Chem.—Eur. J.* **2007**, *13*, 8928−8938.
(33) (a) Ding, E.; Liu, F.-C.; Liu, S.; Meyers, E. A.; Shore, S. G. *Inorg. Chem.* **2002**, *41*, 5329−5335. (b) Chen, X.; Liu, F.-C.; Plečnik, C. E.; Liu, S.; Du, B.; Meyers, E. A.; Shore, S. G. *Organometallics* **2004**, *23*, 2100−2106. (c) Ding, E.; Du, B.; Liu, F.-C.; Liu, S.; Meyers, E. A.; Shore, S. G. *Inorg. Chem.* **2005**, *44*, 4871−4878. (d) Ding, E.; Du, B.; Shore, S. G. *J. Organomet. Chem.* **2007**, *692*, 2148−2152. (e) Hamilton, E. J. M.; Park, J. S.; Chen, X.; Liu, S.; Sturgeon, M. R.; Meyers, E. A.; Shore, S. G. *Organometallics* **2009**, *28*, 3973−3980.
(34) The K_{eq} value is the average of three experiments.
(35) For covalent radius data of Ni (1.24 ± 0.04 Å) and B (0.84 ± 0.03 Å), see: Cordero, B.; Gómez, V.; Platero-Prats, A. E.; Revés, M.; Echeverría, J.; Cremades, E.; Barragán, F.; Alvarez, S. *Dalton Trans.* **2008**, 2832−2838.
(36) For details, see Supporting Information of ref 1.
(37) Catecholborane has a boiling point of 50 °C at 50 mmHg.
(38) *Modern Physical Organic Chemistry*; Anslyn, E. V., Dougherty, D. A.; University Science Books: Sausalito, CA, 2004; pp 432−433.
(39) Rablen, P. R.; Hartwig, J. F. *J. Am. Chem. Soc.* **1996**, *118*, 4648−4653.

(40) (a) Tilset, M. Organometallic Electrochemistry: Thermodynamics of Metal-Ligand Bonding. In *Comprehensive Organometallic Chemistry III*; Crabtree, R. H., Mingos, D. M. P., Eds.; Elsevier: Oxford, U.K., 2007; Vol. *1*, pp 279−305. (b) Choi, J.; Pulling, M. E.; Smith, D. M.; Norton, J. R. *J. Am. Chem. Soc.* **2008**, *130*, 4250−4252.
(41) Bush, R. C.; Angelici, R. J. *Inorg. Chem.* **1988**, *27*, 681−686.
(42) Pandarus, V.; Zargarian, D. *Organometallics* **2007**, *26*, 4321−4334.
(43) Kramer, G. W.; Brown, H. C. *J. Organomet. Chem.* **1974**, *73*, 1−15.
(44) Köster, R.; Tsay, Y.-H.; Krüger, C.; Serwatowski, J. *Chem. Ber.* **1986**, *119*, 1174−1188.

dx.doi.org/10.1021/ic300587b | *Inorg. Chem.* 2013, 52, 37−47